

INFLUENCE OF LEAD NANOPARTICLES ON STRUCTURAL, MORPHOLOGICAL, AND MECHANICAL CHARACTERISTICS OF (SiR-PU/Micro-Pb) COMPOSITES FOR RADIATION SHIELDING APPLICATIONS[†]

✉ Mousa Hawan Naeem^{a,*}, ✉ Sameer Hassan Hadi Al-Nesrawy^a, ✉ Mohammed H. Al-Maamori^b

^aDepartment of Physics, College of Education for Pure Sciences, University of Babylon, Al-Hilla, 51001, Iraq

^bDepartment of Bio-Medical Engineering, College of Engineering, University of Al-Mustaqbal, Babylon, Al-Hilla, 51001, Iraq

*Corresponding Author e-mail: mousahawannaem@gmail.com

Received April 21, 2023; revised June 19, 2023; accepted June 19, 2023

This research includes the manufacture of a polymeric nanocomposite consisting of silicone rubber/polyurethane as a base, with the addition of the first filler of micro-lead with a ratio of 300 pphr and the second filler of nano-lead with different ratios (0, 0.2, 0.4, 0.6, 0.8 pphr). With the addition of hexane (liquid state) to the superposition using the casting technique at room temperature. The structural properties of the surfaces of the samples were measured using Fourier transformation spectroscopy (FT-IR) and the scanning electron microscope (SEM). In addition to studying the mechanical properties represented by each hardness, tensile, elongation, and elastic modulus. (FT-IR) showed the absence of a chemical reaction for all samples. While SEM measurements showed a homogeneous distribution of micro-lead and nano-lead in the presence of hexane equally, and there were no voids in the eyes of the prepared rubber equally. For the mechanical properties, we see that the hardness, tensile strength and modulus of elasticity continue to improve with the increase in the number of lead nanoparticles. And a decrease in elongation as a result of inverse proportion to the modulus of elasticity. From the results obtained, this composite can be used in gamma ray attenuation applications in shielding, especially in medical and industrial fields.

Keywords: Mechanical characteristics; Silicone rubber; Polyurethane; lead; Hexane; SiR-PU/micro-Pb/nano-Pb nanocomposites

PACS: 61.25.he, 68.35.B, 68.37.Hk, 68.60.Bs, 28.41.Qb

1. INTRODUCTION

A composite material is made of two or more different materials that are put together at a macroscopic level to create new qualities that can't be made by the parts working alone. Each material has its own chemical, physical, and mechanical qualities, unlike metal alloys [1]. Composites are made up of a reinforcing component and a matrix phase. Materials like polymers, ceramics, and metals can serve as the matrix phase, while fibers, flakes, or particles provide the reinforcing phase with the greater strength and stiffness. Most of the time, composite materials are put into four groups: fibrous composites, laminated composites, particle composites, and others [2]. The potential of composites as a strengthening material for many issues related to infrastructure deterioration has only recently become apparent to civil engineers and the building industry [3]. Composites are made by combining different materials that all have useful mechanical and physical characteristics [4]. In numerous engineering applications, the use of massive metals decreases the product's performance. Due to their high specific stiffness and strength, polymer-based synthetic fibre composites began to be used in numerous applications in 1930 to surmount this limitation [5]. The goal of making hybrid composites is to improve the composite characteristics by using multiple reinforcing agents in a single polymer matrix. The reinforcement impact can be enhanced or diminished depending on whether multiple reinforcing materials are used together [6]. Silicone rubber is a widely used manufactured elastomer because of its high quality and versatility. Silicone rubber can be subdivided into various kinds based on differences in monomer, vulcanization conditions, applicable environments, etc. [7]. Silicone rubber's molecular framework was built from Si-O links that alternated with one another. The primary cause of silicone rubber's deterioration with age was the breakdown of its molecular structure in a hot atmosphere. There were two major categories to the aging mechanism of silicone rubber in a thermal oxygen environment. A rearrangement process was initiated, on the one hand, due to the breaking of the Si-O-Si bond. However, the silicone rubber molecule chain structure was altered due to the oxidation of side groups [7]. Polyurethanes (PU) can be found in a wide variety of contemporary products. They are a type of polymer that has found extensive application in the healthcare, transportation, and manufacturing sectors. Polyurethanes can be found in a wide variety of goods, including furniture, coatings, adhesives, building materials, fibers, paddings, paints, elastomers, and synthetic skins [8]. Today's catheters are typically made from polyurethane or silicon elastomer. Catheter-related bloodstream infections and thrombotic complications happened significantly more frequently with polyurethane catheters in a study comparing 698 venous-access ports implanted at the forearm made of both materials. However, mechanical failures like disconnection and catheter breakage are on the rise in silicon. However, this finding only applies to devices and catheters inserted through a brachial port, which are subjected to distinct mechanical forces than those experienced through a chest port. Rubber may have an effect on catheter-related complications, as evidenced by the fact that significant differences were observed with regard to the used catheter material [9]. Because effective radiation protection materials are readily available, it is possible to use technologies that generate ionizing radiation, such as gamma rays and radioactive sources, without risking one's health. In this context, advancements in efficacious radiation shielding materials have

[†] Cite as: M.H. Naeem, S.H.H. Al-Nesrawy, M.H. Al-Maamori, East Eur. J. Phys. 3, 539 (2023), <https://doi.org/10.26565/2312-4334-2023-3-63>

© M.H. Naeem, S.H.H. Al-Nesrawy, M.H. Al-Maamori, 2023

gained a significant importance, which motivates the researchers working in the field of nuclear radiation to continuously search and fabricate new radiation, some of these studies are focused on developing composite materials by incorporation of various filler materials in various matrices so that the various properties of these materials will be merged and one effective composite radiation shield will be formed. In this respect, polymers are a good example because they are highly valued matrix materials that can be used to develop gamma-ray barriers that are light weight, resilient, and malleable [10,11]. Nano-particles due to extraordinary characteristics including a high surface-to-volume ratio, are incorporated into the polymer matrices to make polymer-nanocomposites that have a wide range of applications for dosimetry, calorimetric, and radiation protection purposes especially for diagnostic X-rays [12]. Silicon rubber matrix with nanomaterials can improve the gamma radiation attenuation characteristics of nanocomposites because nanomaterials are more uniform and exert less force in the composite, thereby enhancing the material's protective capacity [13]. Many fields, including manufacturing quality control, basic science, astronomy, astrophysics, nuclear engineering, medicine, and even space exploration, have made significant use of X-ray and gamma-ray technology. However, due to long-term exposure, ionizing radiation can be harmful to people working in the field, to equipment, and to the ecosystem. Shielding is the most efficient way to block harmful rays in radiation uses. Since lead is the most commonly used material for radiation shielding, its toxicity, weight, and disposal issues have severely constrained its application. As a result, alloys and glasses have been developed as progressively more suitable replacements [14]. In this present work, polymer nanocomposites were synthesized and its structural, mechanical and radiation properties were measured. From the unique results obtained, it can be used in shielding applications, especially in the medical and industrial fields.

2. MATERIALS AND METHODS

The materials used in the present work are silicone rubber and polyurethane as matrix, while micro-lead and nanoparticles are used as additives; a sensitive electrical scale for weighing small amounts of samples [15] with a hardness measuring instrument for measuring the rubber's hardness [16]; the (Shore-A) hardness tester (H-17A, Congenix-Wallac) tested hardness experimentally, English (Kingston) [17]. Silicone rubber is combined with a specific amount of (SiR₈₀pphr-PU₂₀pphr/micro-pb₃₀₀pphr) nano-Pb powder (99.5% purity, 50 nm diameter) is then doped at quantities of (0, 0.2, 0.4, 0.6, 0.8 pphr) where the mixture was stirred for 15 minutes using a Stirrer (HT-120DX) and hexane to fill the gaps and homogenise the lead material by casting, to make nanocomposites of (SiR₈₀/PU₂₀/micro-pb₃₀₀/nano-pb_{0.8}). The rubber samples were tested by Fourier infrared spectroscopy (FT-IR) with the wavelength range (600-4000) cm⁻¹ [18]. Scanning Electron Microscope (SEM) and measuring some mechanical characteristics of rigidity represented by the hardness, tensile, elongation and modulus of elastic [19]. And radiation characteristics using two elements, Cs137 and Co60, by an American-made Geiger counter [20].

3. RESULT AND DISCUSSION

Figure 1 represents the FT-IR spectra of the rubber composite of (SiR₈₀/PU₂₀/micro-pb₃₀₀/nano-pb_{0.8}), with hexane in the rang (600-4000) cm⁻¹, where it was observed that there are no apparent changes in the radiation spectrum. Infrared for the rubber composite [21].

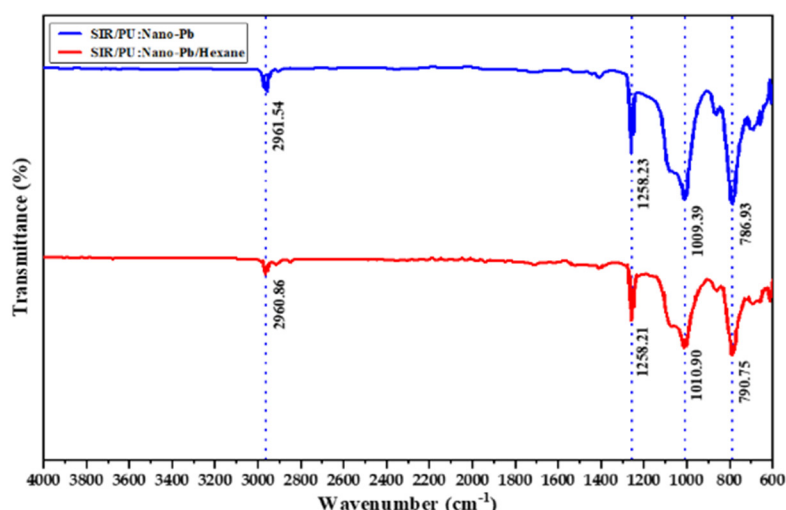


Figure 1. Plot of rubber composite (SiR₈₀/PU₂₀/micro-Pb₃₀₀/nano-Pb_{0.8}) of the sample without hexane and within hexane

Even when the loading ratios changed, the presence of hexane closed the gaps in the rubber composite, and the lead distribution was equally distributed. The FTIR spectra displayed the unique bonds of vibrations. The FTIR spectra displayed the distinctive bonds of vibrations. These spectra of silicone rubber's distinctive peaks stretch from the functional groups generated in the composites when the crosslinker weight ratio increased. Absorption peaks at 1258.4 cm⁻¹, 790.75 cm⁻¹, and 1010.90 cm⁻¹ were attributable to methyl groups and Si-O bonds, respectively. The results

suggested that methyl groups on the side-chain were degraded during the corona process and the polymer main-chain became decomposed [22].

Figure 2. The sample consisting of (SiR₈₀/PU₂₀/micro-pb₃₀₀/nano-pb_{0.8}) was viewed on a scanning electron microscope (SEM) (Hitachi, Japan) before mixing the hexane. Image (B) shows lead heterogeneity and voids in the composite sample, while image (A) shows nanoparticles evenly distributed and no voids after mixing hexane. The two images are the same and have the same components and amounts [23-25]. Figure 3 shows the distribution function in numbers (B, B1), the diameter and area of the nanolead volume without hexane, and (A, A1), the diameter and volume area of the nano lead with hexane. This shows that the nano lead is evenly distributed over the sample. The polymeric chains crosslinked in image (A, A1) [26-27].

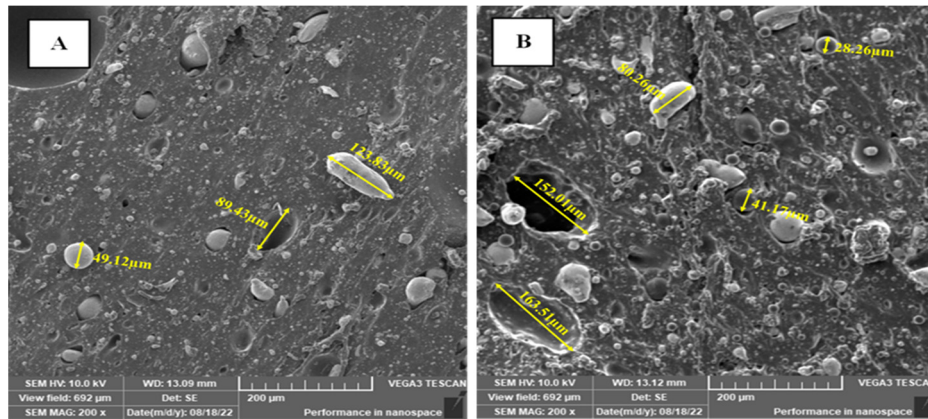


Figure 2. SEM image of: (A) when hexane is added, and (B) the sample without hexane

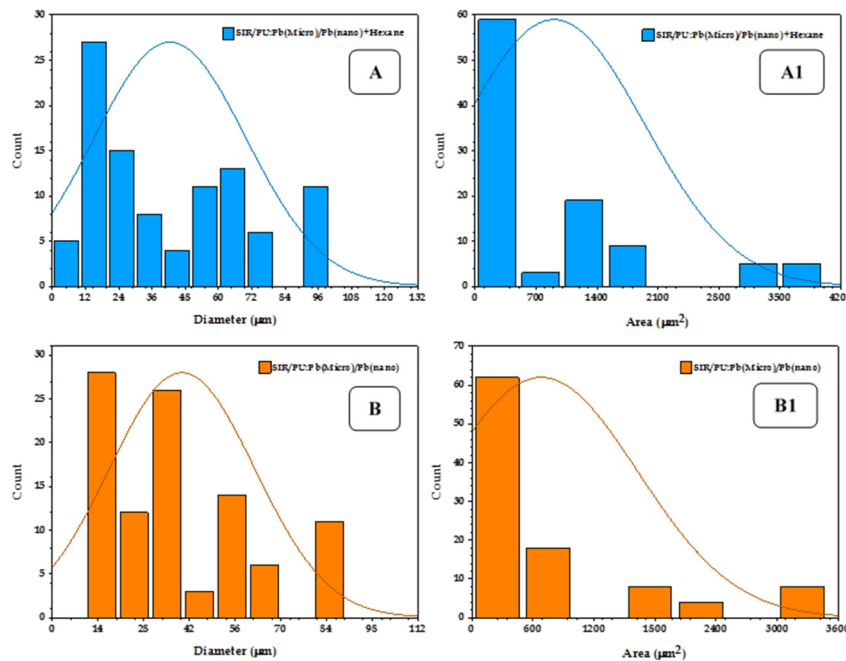


Figure 3. Plot of particles distributive function for (A, A1) represents the diameter and volume area of Nano-lead when hexane is added. (B, B1) represent the diameter and volume area of Nano-lead without adding hexane.

Table 1 represents the components of all batches of the composite (SiR₈₀/PU₂₀/micro-pb₃₀₀) with different weight ratios of Nano-Pb (0, 0.2, 0.4, 0.6, 0.8 pphr). Table 2 represents the results of examining the mechanical properties of hardness, tensile strength, elongation, and modulus of elasticity.

Table 1. Represented by fixed weight ratios of (SiR/PU/micro-Pb) with different weight ratios of (nano-Pb)

Sample No	SiR ₈₀ (pphr) + PU ₂₀ (pphr)	(micro-pb) (pphr)	(Nano-pb) (pphr)
Sam 1	100	300	0
Sam 2	100	300	0.2
Sam 3	100	300	0.4
Sam 4	100	300	0.6
Sam 5	100	300	0.8

Table 2. Represents the results of the mechanical characteristics examination represented by hardness, tensile, elongation and modulus of elasticity.

Sample No	Hardness (Shore A)	Tensile Strength (Mpa)	Elongation at %	Elastic Modulus (Mpa)
Sam 1	29.7	0.544	127.5	4.2×10^{-3}
Sam 2	30.1	0.564	125.5	4.4×10^{-3}
Sam 3	32.5	0.577	120.5	4.7×10^{-3}
Sam 4	34.0	0.597	117.5	5.0×10^{-3}
Sam 5	34.7	0.614	113.5	5.4×10^{-3}

Figure 4. It is clear that the measured hardness values for the surface of the rubber doughs increased gradually and irregularly with the increase in the amount of the additive (Nano-Pb). The reason for this is due to the interference that occurs between the supporting material and the base material, which increases the value of the hardness. The reason for this is due to the occurrence of some cross-linking between the rubber chains and the additive inside the prepared dough that is responsible for resisting the external forces applied to it, which increases the hardness of the surface of the prepared material and this agrees with previous research [28].

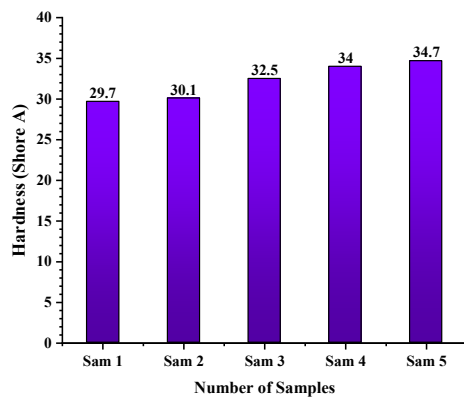


Figure 4. Plot of change the hardness for different blends samples

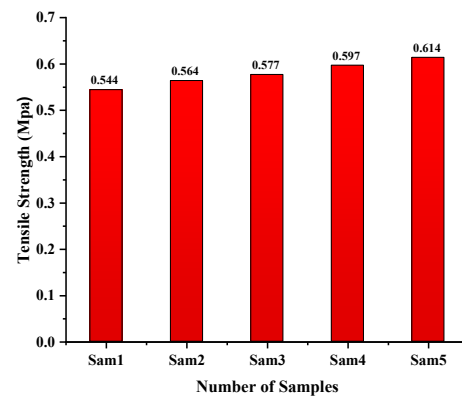


Figure 5. Plot of change the tensile strength for different blends samples

Figures 5, 6 and 7 show the effect of Nano-lead powder additive with loading ratios (0,0.2,0.4,0.6,0.8 pphr) on some mechanical characteristics such as tensile, modulus of elasticity and elongation of the rubber composite consisting of silicone rubber (80). and polyurethane (20) for rubber batches, and as a result of the comparison between the effects of mechanical tests (tensile resistance, modulus of elasticity and elongation) as well as the radiation characteristics of the batches models [29].

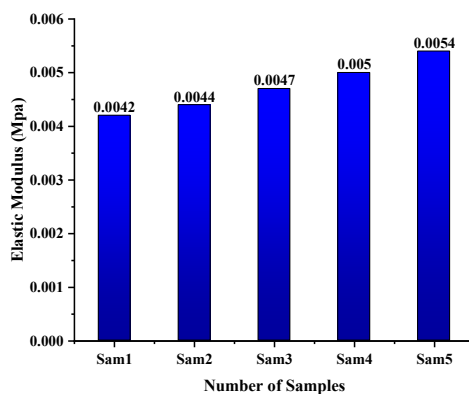


Figure 6. Plot of change the elastic modulus for different blends samples.

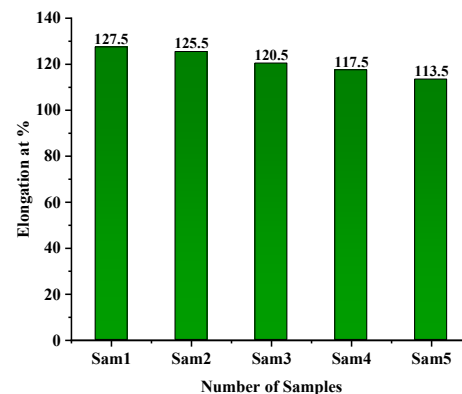


Figure 7. Represents change the elongation for different blends samples

The sample (5) with components (SiR₈₀/PU₂₀/micro-pb₃₀₀) with (nano-pb_{0.8}) pphr was more appropriate. It achieved the mechanical characteristics as we notice from the figures a slight increase in the tensile strength, modulus of elasticity and a decrease in the amount of elongation with the increase in the loading ratio of the Nano-lead powder [30]. This is due to the rise in the physical bonding and the cohesion of the filler with rubber. The Nano lead powder (Pb-nano) has a small granular size that increases the surface area for diffusion and, thus, the formation of a larger amount of crosslinking with the rubber chains, and this is consistent with previous research [31]. It is also noted from the numbers that the decrease in the elongation diagram is explained based on the material's arrival to the point of application, where the

material continues to resist until its resistance collapses as a result of the lack of space between the rubbers. The chains, as they are in a certain percentage, do not bear the added material, which leads to cracks and toxins in the sample. Flexibility, and this is consistent with previous research [32]. As for the increase in the modulus of elasticity, it can indicate a strong drop in elongation, and as a result of its inverse proportion to the modulus of elasticity property [33]. Due to the obvious increase in the modulus of elasticity and tensile strength, the loading percentage of the nano-additive material is increased.

Figure 8 shows the graphical relationship between thickness and penetrating radiation (N) when using a Cs¹³⁷ radiation source and different loading ratios of (Pb-nano). Where a decrease in the value of the thickness of the half X_{1/2} and an increase in both linear and mass absorption coefficients were observed with increasing loading ratios. This is due to the efficiency of the prepared composite in absorbing and attenuating the rays used, and this efficiency increases with increasing the loading percentage of lead nano powder [34] (see Table 3.). From equations (1,2) we obtain the linear absorption coefficient (μ) and the mass (μ_m).

$$\mu = \frac{\ln 2}{X_{1/2}} \tag{1}$$

$$\mu_m = \frac{\mu}{\rho} \tag{2}$$

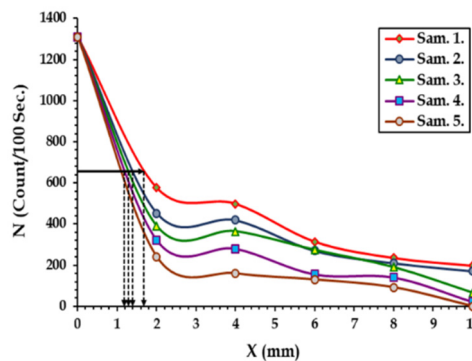


Figure 8. Graphical relationship between thickness and the number of penetrating radiation (N) when using a source (Cs¹³⁷) for different loading ratios of (Pb-nano).

Table 3. Linear and mass absorption coefficient and half thickness of cesium source Cs¹³⁷ for different loading ratios of Pb-nano powder for rubber samples.

Batch No	Nano-Pb	X _{1/2} (mm)	μ (cm ⁻¹)	μ _m (cm ² /gm)
A	0	1.678	4.131	1.487
B	0.2	1.390	4.987	1.622
C	0.4	1.288	5.381	1.723
D	0.6	1.178	5.887	1.877
E	0.8	1.186	5.842	1.861

Figure 9 represents the results obtained for the Co⁶⁰ cobalt source. The second source of electromagnetic radiation, the Co⁶⁰ source, was used to examine the superimposed rubber models. We observed a decrease in the thickness of the half when the percentage of additive loading was increased. Basically about the number of particles in the radiation path [35], see Table 4.

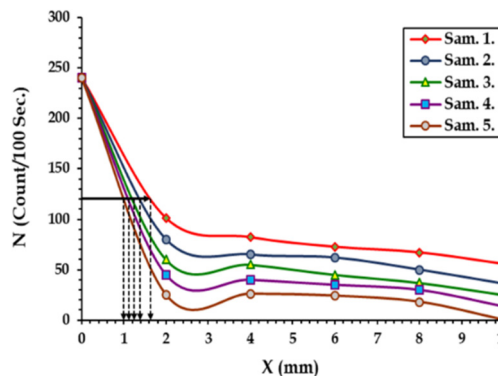


Figure 9. Graphical relationship between thickness and the number of penetrating radiation (N) when using a source (Co⁶⁰) for different loading ratios of (Nano-Pb)

Table 4. Linear and mass absorption coefficient and half thickness of cobalt source Co⁶⁰ for different loading ratios of nano-Pb powder for rubber samples.

Batch No	Nano-Pb	X _{1/2} (mm)	μ (cm ⁻¹)	μ _m (cm ² /gm)
A	0	1.624	4.269	1.537
B	0.2	1.389	4.991	1.623
C	0.4	1.234	5.616	1.799
D	0.6	1.108	6.253	1.994
E	0.8	0.985	7.040	2.243

4. CONCLUSIONS

The purpose of this research is to better understand the characteristics of (SiR₈₀/PU₂₀/micro-pb₃₀₀/nano-pb_{0.8}) nanostructures for use as radiation shielding in the medical and industrial fields. These findings from our study allow us to conclude:

1- When nano lead powder was added to the batch for the prepared composite of (SiR₈₀/PU₂₀/micro-Pb₃₀₀) with a ratio of (0.8pphr) on the mechanical properties, it led to an increase in tensile strength, hardness modulus and modulus of elasticity with a decrease in elongation.

2- The prepared rubber batch samples were examined with the FTIR device, and it was noted that there was no change in the rubber composites and We gradually obtained a physical correlation in all the composites.

3- Also, the rubber batch samples examined by the (SEM) device were examined, as the lead was distributed evenly, and there were no voids on the samples prepared in the presence of hexane.

4- The lowest thickness and the largest linear and mass absorption coefficients were obtained at the loading ratio of 300 pphr and 0.8 pphr when using the Co⁶⁰ source.

5- The samples were tested for attenuation of radiation from the sources Cs¹³⁷ and Co⁶⁰ whose decay energy is 1.17563 MeV and 2.82307 MeV, respectively. The results indicated that the linear absorption coefficient (μ) and mass absorption coefficient (μ_m) are continually growing, while the half-thickness (X_{1/2}) is decreasing with ray attenuation.

6- The sample was selected (SiR₈₀/PU₂₀/micro-Pb₃₀₀/nano-Pb_{0.8}) it can be used in armor applications as an armor suit to protect workers in the medical and industrial fields.

Acknowledgements

We thank university of Babylon for their great support to complete this work.

ORCID

©Mousa Hawan Naeem, <https://orcid.org/0000-0002-3508-3606>; ©Sameer Hassan Hadi Al-Nesrawy, <https://orcid.org/0009-0001-2888-7980>; ©Mohammed H. Al-Maamori, <https://orcid.org/0009-0004-7543-9883>

REFERENCE

- [1] J. Cai, L. Qiu, S. Yuan, *et al.*, "Structural health monitoring for composite materials," in: Composites and Their Applications, edited by N. Hu, Intech, (2012). <https://doi.org/10.5772/3353>
- [2] T. Singh, and S. Sehgal, "Structural health monitoring of composite materials," Arch. Comput. Methods Eng. **29**, 1997-2017 (2022). <https://doi.org/10.1007/s11831-021-09666-8>
- [3] S.S. Pendhari, T. Kant, and Y.M. Desai, "Application of polymer composites in civil construction: A general review," Compos. Struct. **84**, 114-124 (2008). <https://doi.org/10.1016/j.compstruct.2007.06.007>
- [4] R. Hsissou, R. Seghiri, Z. Benzekri, M. Hilali, M. Rafik, and A. Elharfi, "Polymer composite materials: A comprehensive review," Compos. Struct. **262**, 113640 (2021). <https://doi.org/10.1016/j.compstruct.2021.113640>
- [5] S.O. Prakash, P. Sahu, M. Madhan, A.J. Santhosh, "A review on natural fibre-reinforced biopolymer composites: properties and applications," Int. J. Polym. Sci. **2022**, 7820731 (2022). <https://doi.org/10.1155/2022/7820731>
- [6] N.I.N. Haris, M.Z. Hassan, R.A. Ilyas, M.A. Suhot, S.M. Sapuan, R. Dolah, R. Mohammad, *et al.*, "Dynamic mechanical properties of natural fiber reinforced hybrid polymer composites: A review," J. Mater. Res. Technol. **19**, 167-182 (2022). <https://doi.org/10.1016/j.jmrt.2022.04.155>
- [7] R. Han, Y. Li, Q. Zhu, and K. Niu, "Research on the preparation and thermal stability of silicone rubber composites: A review," Compos. Part. C, **100249** (2022). <https://doi.org/10.1016/j.jcom.2022.100249>
- [8] G.T. Howard, "Biodegradation of polyurethane: a review," Int.. Biodeterior. Biodegradation, **49**, 245-252 (2002). [https://doi.org/10.1016/S0964-8305\(02\)00051-3](https://doi.org/10.1016/S0964-8305(02)00051-3)
- [9] U. Braun, E. Lorenz, C. Weimann, H. Sturm, I. Karimov, J. Ettl, R. Meier, *et al.*, "Mechanic and surface properties of central-venous port catheters after removal: A comparison of polyurethane and silicon rubber materials," J. Mech. Behav. Biomed. Mater. **64**, 281-291 (2016). <https://doi.org/10.1016/j.jmbbm.2016.08.002>
- [10] O. Kiliçoglu, C.V. More, F. Akman, K. Dilsiz, H. Oğul, M.R. Kaçal, H. Polat, *et al.*, "Micro Pb filled polymer composites: Theoretical, experimental and simulation results for γ-ray shielding performance," Radiat. Phys. Chem. **194**, 110039 (2022). <https://doi.org/10.1016/j.radphyschem.2022.110039>
- [11] M.Ö. Kiliçoglu, "Micro Pb filled polymer composites: Theoretical, experimental and simulation results for gamma-ray shielding performance," (2022). <https://openaccess.marmara.edu.tr/bitstreams/4c3b39bc-86a4-4e63-b3d5-59ed74fabd3b/download>
- [12] M.A. Hosseini, S. Malekie, F. Kazemi, "Experimental evaluation of gamma radiation shielding characteristics of polyvinyl alcohol/tungsten oxide composite: A comparison study of micro and nano sizes of the fillers," Nucl. Instruments. Methods Phys. Res. Sect. A, Accel. Spectrometers, Detect. Assoc. Equip. **1026**, 166214 (2022). <https://doi.org/10.1016/j.nima.2021.166214>
- [13] El-Khatib A.M., Abbas M.I., Hammoury S.I., *et al.*, "Effect of PbO-nanoparticles on dimethyl polysiloxane for use in radiation shielding applications," Sci. Rep. **12**, 15722 (2022). <https://doi.org/10.1038/s41598-022-20103-z>
- [14] J. Wu, J. Hu, K. Wang, Y. Zhai, Z. Wang, Y. Feng, H. Fan, *et al.*, "Flexible stretchable low-energy X-ray (30–80 keV) radiation shielding material: Laser-melting-point GaIn1Sn7Bi1 alloy/thermoplastic polyurethane composite," Appl. Radiat. Isot. **192**, 10603 (2023). <https://doi.org/10.1016/j.apradiso.2022.110603>

- [15] Román A.J., Qin S., Rodríguez J.C., L.D. González, V.M. Zavala, and T.A. Osswald, "Natural rubber blend optimization via data-driven modeling: The implementation for reverse engineering," *Polymers*, (Basel), **14**, 2262 (2022). <https://doi.org/10.3390/polym14112262>
- [16] A. Umanskii, K. Gogolinskii, V. Syasko, and A. Golev, "Modification of the Leeb Impact Device for Measuring Hardness by the Dynamic Instrumented Indentation Method," *Inventions*, **7**, 29 (2022). <https://doi.org/10.3390/inventions7010029>
- [17] Y. Wang, C. Feng, M. Zhao, C. Shan, F. Liu, Q. Lei, Z. Zhou, *et al.*, "Development of a high energy resolution and wide dose rate range portable gamma-ray spectrometer," *Appl. Radiat. Isot.* **192**, 110572 (2023). <https://doi.org/10.1016/j.apradiso.2022.110572>
- [18] Lilo T., Morais C.L.M., Shenton C., *et al.*, "Revising Fourier-transform infrared (FT-IR) and Raman spectroscopy towards brain cancer detection," *Photodiagnosis. Photodyn. Ther.* **102785** (2022). <https://doi.org/10.1016/j.pdpdt.2022.102785>
- [19] T. Marquardt, and A.W. Momber, "The assessment of fractal dimensions with the direct use of scanning electron microscopy (SEM) images from blast-cleaned steel substrates," *J. Adhes. Sci. Technol.* **37**, 16–37 (2023). <https://doi.org/10.1080/01694243.2021.2013057>
- [20] Libeesh N.K., Naseer K.A., Arivazhagan S., *et al.*, "Multispectral remote sensing for determination the Ultra-mafic complexes distribution and their applications in reducing the equivalent dose from the radioactive wastes," *Eur. Phys. J. Plus.* **137**, 267 (2022). <https://doi.org/10.1140/epjp/s13360-022-02473-5>
- [21] M.H. Naeem, and S.H.H. Al-Nesrawy, "Preparation of (Rubber Blend/Oyster Shell Powder) Composites and Study Rheological Properties," *J. Engineer. Appl. Sciences*, **14**(7), 10092-10097 (2019). <https://dx.doi.org/10.36478/jeasci.2019.10092.10097>
- [22] Y. Yang, Z. Wang, X. Peng, Z. Huang, and P. Fang, "Influence of Crosslinking Extent on Free Volumes of Silicone Rubber and Water Diffusion after Corona Discharge," *Materials* (Basel), **15**, 6833 (2022). <https://doi.org/10.3390/ma15196833>
- [23] S.H.K. Bahrain, N.R.N. Masdek, J. Mahmud, M.N. Mohammed, S.M. Sapuan, R.A. Ilyas, A. Mohamed, *et al.*, "Morphological, physical, and mechanical properties of Sugar-Palm (Arenga pinnata (Wurmb) Merr.)-Reinforced silicone rubber biocomposites," *Materials* (Basel), **15**, 4062 (2022). <https://doi.org/10.3390/ma15124062>
- [24] M.H. Meteab, A. Hashim, and B.H. Rabee, "Controlling the Structural and Dielectric Characteristics of PS-PC/Co2O3-SiC Hybrid Nanocomposites for Nanoelectronics Applications," *Silicon*, **15**, 251-261 (2023). <https://doi.org/10.1007/s12633-022-02020-y>
- [25] M.H. Meteab, A. Hashim, B.H. Rabee, "Synthesis and Characteristics of SiC/MnO2/PS/PC Quaternary Nanostructures for Advanced Nanodielectrics Fields," *Silicon*, **15**, 1609-1620 (2023). <https://doi.org/10.1007/s12633-022-02114-7>
- [26] T.L. Christiansen, S.R. Cooper, and K.M.Ø. Jensen, "There's no place like real-space: elucidating size-dependent atomic structure of nanomaterials using pair distribution function analysis," *Nanoscale Adv.* **2**, 2234-2254 (2020). <https://doi.org/10.1039/D0NA00120A>
- [27] H.S. Suhail, and A.R. Abdulridha, "Investigation of the Morphological, Optical, and D.C Electrical Characteristics of Synthesized (Bi₂O₃/ZnO) Nanocomposites, as Well as Their Potential Use in Hydrogen Sulfide Gas Sensor," *Trans. Electr. Electron. Mater.* **24**, 205–216 (2023) (2023). <https://doi.org/10.1007/s42341-023-00436-w>
- [28] C. Yang, C. Ren, Y. Jia, G. Wang, M. Li, and W. Lu, "A machine learning-based alloy design system to facilitate the rational design of high entropy alloys with enhanced hardness," *Acta Mater.* **222**, 117431 (2022). <https://doi.org/10.1016/j.actamat.2021.117431>
- [29] S.H. Al-Nesrawy, M. Al-Maamori, and H.R. Jappor, "Effect of mixed of industrial scraps and lamp black percent on the mechanical properties of NR70/SBR30 composite," *Int. J. Pharm. Tech. Res.* **9**, 207-217 (2016).
- [30] A.A. Abid, S.H. Al-Nesrawy, and A.R. Abdulridha, "New fabrication (PVA-PVP-C. B) nanocomposites: structural and electrical properties," *Journal of Physics: Conference Series*, IOP Publishing, **1804**, 012037 (2021). <https://doi.org/10.1088/1742-6596/1804/1/012037>
- [31] Y. Zeng, L. Tang, and Z. Xin, "Improved dielectric and mechanical properties of Ti₃C₂T_x MXene/silicone rubber composites achieved by adding a few boron nitride nanoplates," *Ceram. Int.* **49**(6), 9026-9034 (2023).. <https://doi.org/10.1016/j.ceramint.2022.11.058>
- [32] A. Gupta, K.K. Saxena, A. Bharti, J. Lade, K. Chadha, and P.R. Paresi, "Influence of ECAP processing temperature and number of passes on hardness and microstructure of Al-6063," *Adv. Mater. Process Technol.* **8**, 1635-1646 (2022). <https://doi.org/10.1080/2374068X.2021.1953917>
- [33] A.M. Ajam, S.H. Al-Nesrawy, and M. Al-Maamori, "Effect of reclaim rubber loading on the mechanical properties of SBR composites," *Int. J. Chem. Sci.* **14**, 2439-2449 (2016). <https://www.tsijournals.com/articles/effect-of-reclaim-rubber-loading-on-the-mechanical-properties-of-sbr-composites.pdf>
- [34] E. Timakova, Ms.S. Thesis, "Characterization of Dosimeters for Small Field Applications Including Comparisons to Monte Carlo and Treatment Planning System Computed Doses," McMaster University, (2022). <http://hdl.handle.net/1828/14616>
- [35] H. Al-Ghamdi, M.I. Sayyed, and M. Elsaifi, A. Kumar, N. Al-Harbi, A.H. Almuqrin, S. Yasmin, *et al.*, "An experimental study measuring the photon attenuation features of the P₂O₅-CaO-K₂O-Na₂O-PbO glass system," *Radiat. Phys. Chem.* **200**, 110153 (2022). <https://doi.org/10.1016/j.radphyschem.2022.110153>

**ВПЛИВ НАНОЧАСТИНОК СВИНЦЮ НА СТРУКТУРНІ, МОРФОЛОГІЧНІ ТА МЕХАНІЧНІ
ХАРАКТЕРИСТИКИ (SiR-PU/Micro-Pb) КОМПОЗИТІВ ТА ЗАСТОСУВАННЯ
ДЛЯ ЗАХИСТУ ВІД ВИПРОМІНЮВАННЯ**

Муса Хаван Наем^a, Самір Хасан Хаді Аль-Несраві^a, Мохаммед Х. Аль Мааморі^b

^aКафедра фізики, Освітній коледж чистих наук, Вавилонський університет, Аль-Хілла, 51001, Ірак

^bКафедра біомедицинської інженерії, Інженерний коледж, Університет Аль-Мустакбал, Вавилон, Аль-Хілла, 51001, Ірак

Це дослідження включає виготовлення полімерного нанокompозиту, що складається із силіконового каучуку/поліуретану як основи, з додаванням першого наповнювача з мікросвинцю із співвідношенням 300 phr та другого наповнювача з наносвинцю з різними співвідношеннями (0, 0,2, 0,4, 0,6, 0,8 phr). З додаванням гексану (рідкий стан) до суперпозиції методом лиття при кімнатній температурі. Структурні властивості поверхонь зразків вимірювали за допомогою спектроскопії з перетворенням Фур'є (FT-IR) та скануючого електронного мікроскопа (SEM). Також вивчалися механічні властивості, а саме твердість, розтягування, відносне подовження та модуль пружності. (FT-IR) показав відсутність хімічної реакції для всіх зразків. У той час як SEM вимірювання показали рівномірний розподіл мікро- та нано-свинцю в присутності гексану, і відсутність пор в підготовленій гумі. Стосовно механічних властивостей спостерігалось, що твердість, межа міцності та модуль пружності покращувалися зі збільшення кількості наночастинок свинцю і зменшення подовження в результаті обернено пропорційно модулю пружності. З отриманих результатів видно що ця сполука може бути використана для ослаблення гамма-випромінювання, особливо в медицині та промисловості.

Ключові слова: механічні характеристики; силіконова гума; поліуретан; свинець; гексан; SiR-PU/мікро-Pb:нано-Pb нанокompозити